Results of use of heat flux sensors on liquid hydrogen tanks

W L Johnson[1], R Balasubramaniam[1,2], and R Hibbs[3,4]

[1]Glenn Research Center, Cleveland, OH 44135 USA
[2]Case Western Reserve University, Cleveland, OH 44106 USA
[3]Jacobs Space Exploration Group, Huntsville, AL 35812 USA
[4]Marshall Space Flight Center, Huntsville, AL 35812 USA

E-mail: Wesley.L.Johnson@nasa.gov

Abstract. Heat flux sensors were used to characterize the performance of insulation on the Structural Heat Intercept, Insulation, and Vibration Evaluation Rig (SHIIVER), a large-scale test article designed to simulate upper stage cryogenic propellant tank thermal performance in simulated space environments. Usually, the insulation heat loads are derived from calculations removing all other heat sources and attributing the residual heat load to the insulation system. Testing for SHIIVER included the tank being just insulated with spray-on-foam insulation as well as covering the domes with multilayer insulation while leaving the barrel section insulated with spray-on-foam. Heat flux sensors were located at multiple locations on both domes as well as on the barrel section of the tank. Results from the SHIIVER testing using the heat flux sensors are compared to other calculated heat inputs for both liquid nitrogen and liquid hydrogen testing as a function of tank fill level. Further investigation into the transient nature of the SHIIVER testing including the heat flux sensors provided insight into heat flow patterns that may not have been otherwise seen using temperature sensors and calculated insulation heat loads. While the demonstrated uncertainties in the absolute values in the heat flux sensors are high, the values and the trends match well with other calculation methods. The results of SHIIVER allow for the use of heat flux sensors for measurements of insulation performance and dynamic system thermal response for future applications.

1. Introduction

Cryogenic fluid tanks are usually insulated with multilayer insulation (MLI) to minimize radiative heat loads in a vacuum environment similar to what is experienced on-orbit. MLI is constructed with layers of metallized (aluminum, gold) substrate films (Mylar, Kapton), which act as high reflectivity radiation shields. Low thermal conductivity spacers of several different styles can be used to separate the layers. The total number of layers is variable but can be 50 layers or more for long duration missions. Loss of performance in MLI systems due to joints, seams, attachments, and other design details of the insulation blankets has been recognized as a concern since the introduction of MLI. When attempting to insulate large tanks, even more seams may be required as the tank dimensions exceed the roll widths available for insulation materials.

In order to demonstrate the application of MLI and other technologies on a relative scale for upper stages, NASA has developed the Structural Heat Intercept, Insulation, and Vibration Evaluation Rig (SHIIVER) [1]. One of the objectives of SHIIVER is to demonstrate the benefits of MLI as applied to upper stage hydrogen and oxygen applications. In order to assess the heat loads through MLI, recent boil-off tank testing have relied on accurately calculating the heat load through any structural, fluid, and instrumentation attachments and subtracting those from the total heat load based on boil-off flow rates. However, it was realized that for SHIIVER that this would not provide accurate results. In order to better be able to ascertain the thermal performance of the MLI, it was determined that the addition of heat flux sensors may be able to help give a better interpretation of the MLI heat flows. Additionally, temperature sensors were located on both sides of the spray-on foam insulation (SOFI), under the MLI, as well as on the MLI outer layer.

2. Test Setup

SHIIVER is a 4 meter diameter by 3.88 m tall tank designed to be operated with both liquid hydrogen and liquid nitrogen. An aluminum forward skirt was designed to where it could be cooled with the effluent boil-off vapor or not cooled with the vapor. A stainless-steel structural system, which included an aft skirt, supported the tank within the vacuum chamber. Heat flux sensors were installed in twelve locations on the liquid hydrogen tank wall, four each on the forward dome, barrel section, and aft dome. Figure 1 shows three heat flux sensors installed on one of the tank domes. For all testing, the tank domes and barrel were covered with SOFI with a thickness of approximately 25 mm. After Baseline testing, a 30 layer multilayer insulation (MLI) system was installed on the forward and aft domes (within the boundaries of the skirts) for preacoustic testing. The SHIIVER test setup is fully described by Johnson et. al. [1].

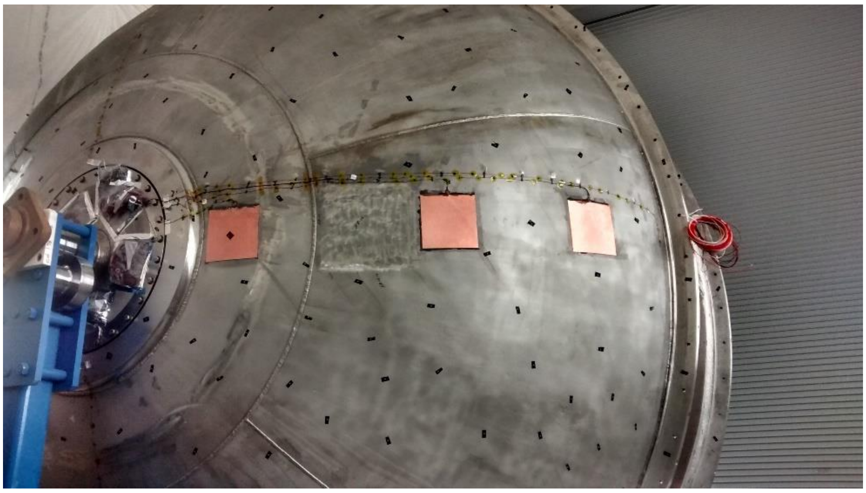

Figure 1. Heat flux sensors installed onto the SHIIVER tank.

2.1. SHIIVER test operations

SHIIVER testing with the MLI installed on the domes was completed both with liquid hydrogen and liquid nitrogen as the test fluid. The liquid hydrogen test consisted of filling the SHIIVER tank to approximately 90% full, and then allowing it to boil-off (through the vent line) until it was less than 25% full. Then the tank was refilled to 90% full and the boil-off routed through the vapor cooling channels and the tank again allowed to boil-off until it reached less than 25% full. For the liquid nitrogen testing, the tank was filled up to 90% full and allowed to boil-off through the vent line to approximately 70% full. Then due to schedule limitation, the tank was refilled to 90% full, with the boil-off routed to the vapor cooling channels. Testing lasted for 48 hours (with the fill level decreasing a few percent) at fill levels of 90%, 50%, and 25% (only a 24 hour test at 25%). This was necessary due to both the slower rate of loss (due to the higher density of nitrogen) and the inability of the test facility to drain the full load of liquid nitrogen at once.

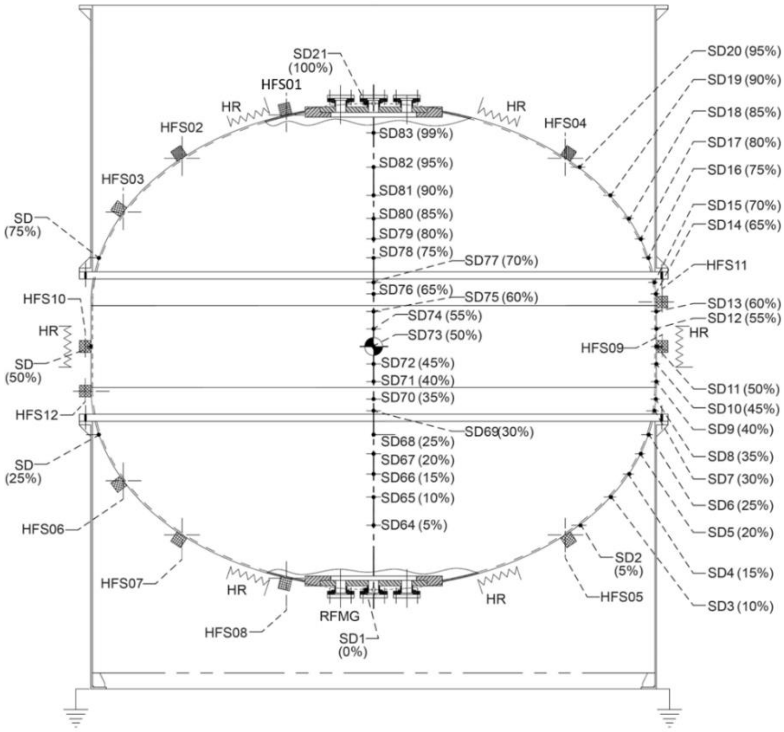

Figure 2. Heat flux sensors installed onto the SHIIVER tank.

Table 1. Heat flux sensor locations, Station location is distance from the tank bottom.

Tank position	Heat flux sensor	Station location, in.	Angular location, θ, degree	Fill level, percent
Forward dome	HFS01	124	225	99
	HFS02	118.1	225	97
	HFS03	100.5	225	86
	HFS04	118.1	45	97
Aft dome	HFS05	10.4	45	3
	HFS06	28.1	225	14
	HFS07	10.4	225	3
	HFS08	0.5	225	0
Tank barrel	HFS09	64.3	45	50
	HFS10	64.3	225	50
	HFS11	76.3	135	63
	HFS12	52.3	315	37

2.2. Heat flux sensors calibration

Heat flux sensor testing and calibration was performed via ASTM C-1130 and ASTM-C1774 on select sensors prior to install onto the SHIIVER test hardware. Results from the testing showed that the published vendor sensitivities were acceptable for use at liquid hydrogen temperatures but had uncertainties on the order of 50%. [2]

The heat flux sensors used are thermopiles, or stacks of multiple thermocouple junctions. The more junctions within the sensor, the higher the differential voltage for a given heat flux and thus a greater sensitivity. While large sensors were used (200 mm x 200 mm), the differential voltage generated by thermocouple junctions at 20 K is low. Thus, at low heat fluxes where temperature differences are low, the uncertainty in the measurements grow significantly.

3. Test Results

Heat flux sensor response is shown for all sensors as a function of time for the forward dome in Figure 3, for the aft dome in Figure 4, and for the barrel in Figure 5. The large breaks in the middle of the timespan indicate the switch from the boil-off testing (occurred first) to the vapor cooling testing (occurred second). Smaller breaks in the timelines indicate self-pressurization testing that generally occurred at 70%, 50%, and 25% during testing (where those fill levels were achieved during testing). Multiple heat flux sensors on the barrel failed (failed to give an output) during various phases of testing, but were able to be fixed prior the next phase of testing. Several sensors on the barrel also started to linearly increase their output over time once the liquid-vapor interface passed the fill level- they were installed at. These sensors recovered during the refill process or in the case of the liquid nitrogen testing, in the middle of the testing. The cause for this trend is not understood.

The heat flux magnitude difference between the multilayer insulation on the domes and the SOFI is clear and of the magnitude expected (approximately two orders of magnitude). The spread between the heat flux sensors is somewhat a surprise, especially on the aft dome. Due to the relative view and environment, one might expect HFS 8 to be the highest flux, with HFS 5 and 7 of similar order due to being at similar locations, only 180 degrees apart, and HFS 6 being closest to the y-joint the lowest. But none of those trends hold. It is also interesting that on the hydrogen test, the heat flux sensors all started out higher and then after the 70% full self-pressurization test, decreased.

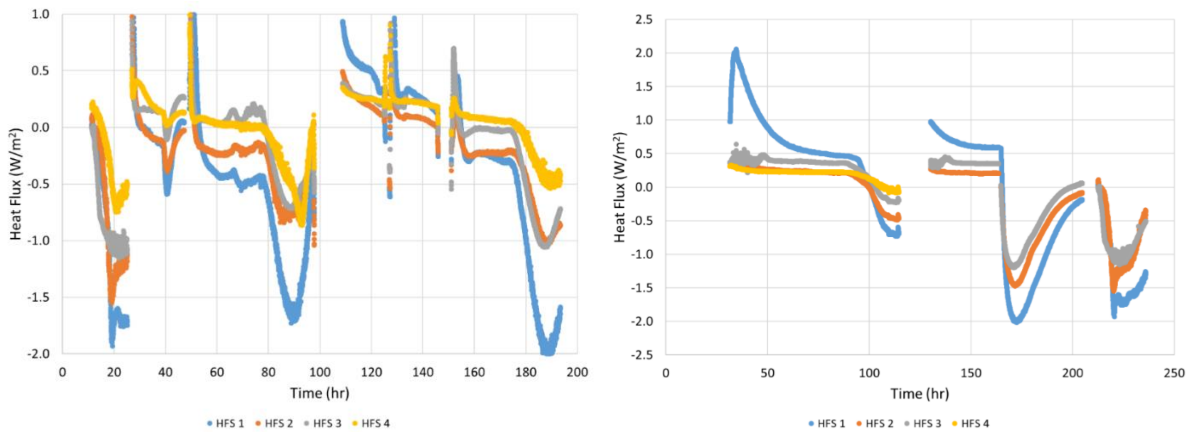

Figure 3. Forward dome heat flux sensor response for Preacoustic liquid hydrogen on left and Preacoustic liquid nitrogen on right.

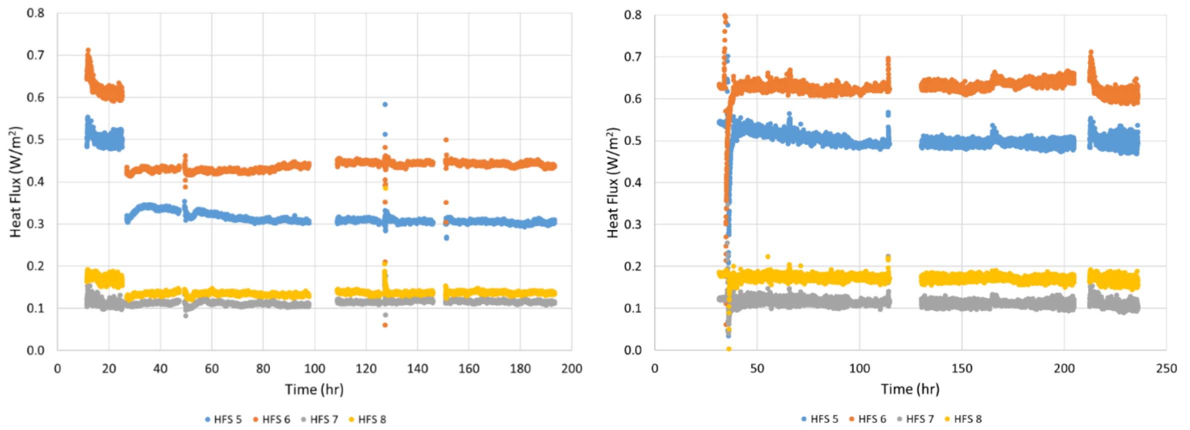

Figure 4. Aft dome heat flux sensor response for Preacoustic liquid hydrogen on left and Preacoustic liquid nitrogen on right.

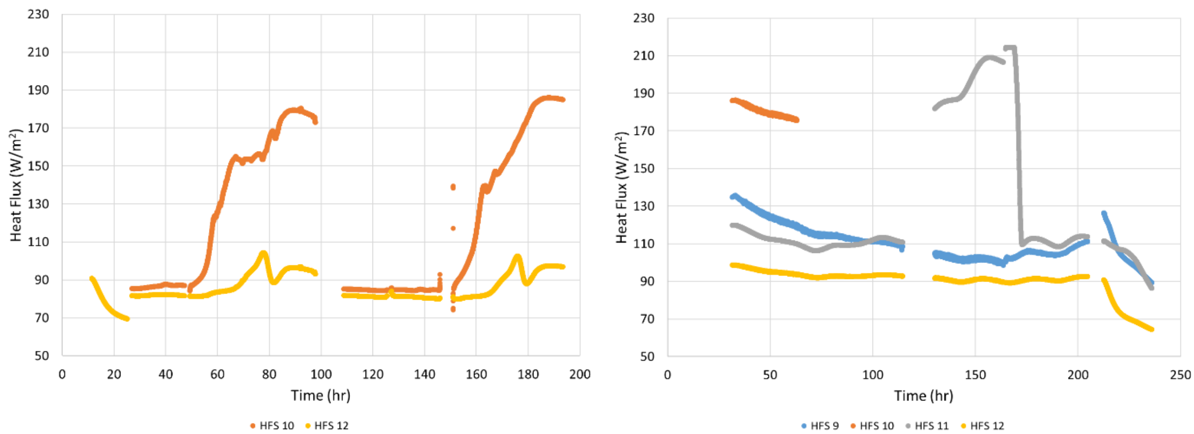

Figure 5. Barrel heat flux sensor response for Preacoustic liquid hydrogen on left and Preacoustic liquid nitrogen on right.

4. Discussion of Results

For comparison to the heat flux sensors, two types of calculations were performed. The first, a "conduction" assessment was performed based on temperature sensor readings across the thickness of the spray-on-foam insulation. The second, a "radiation" assessment was based on the radiative loads and view factors between the test chamber wall and the outer layer of MLI. The plots of all three methods are shown as a function of fill level for the aft dome (figure 6), barrel (figure 7), and forward dome (figure 8). Comparison between the two analysis and measurement on the domes show that the radiation approach is relatively close to the measured heat flux sensor values on the domes where the MLI is present, however the conduction analysis is significantly out of bed with both the measurements and radiation analysis. This discrepancy was attributed to several items: the temperature sensors have a self-heating rate near to or greater than the heat flux coming through the system and the thermal conductivity used for the analysis was not vacuum performance and is also very limited at low temperatures.

Unfortunately, low temperature vacuum performance SOFI data is not readily available. Fesmire [3] and Barrios [4] have previously shown on different materials that there can be significant discrepancies for thermal conductivity, both as a function of temperature and vacuum pressure. Comparison of the approaches on the barrel section shows that all three are much closer in agreement as the SOFI has a warm boundary temperature that is much warmer.

It is also interesting that the heat flux sensors suggest that hydrogen has a lower heat flux than nitrogen, whereas the radiation calculations suggest the opposite. The phenomena of liquid hydrogen MLI performing better than liquid nitrogen MLI has previously been observed on several tests as noted in the initial calibration of the heat flux sensors [2,5,6] and been shown to be feasible when attributed to temperature dependant optical properties within a blanket [7]. However, given the mixed results between the heat flux sensor measurement and radiation calculations in this demonstration and test sequence, there uncertainty to the claim.

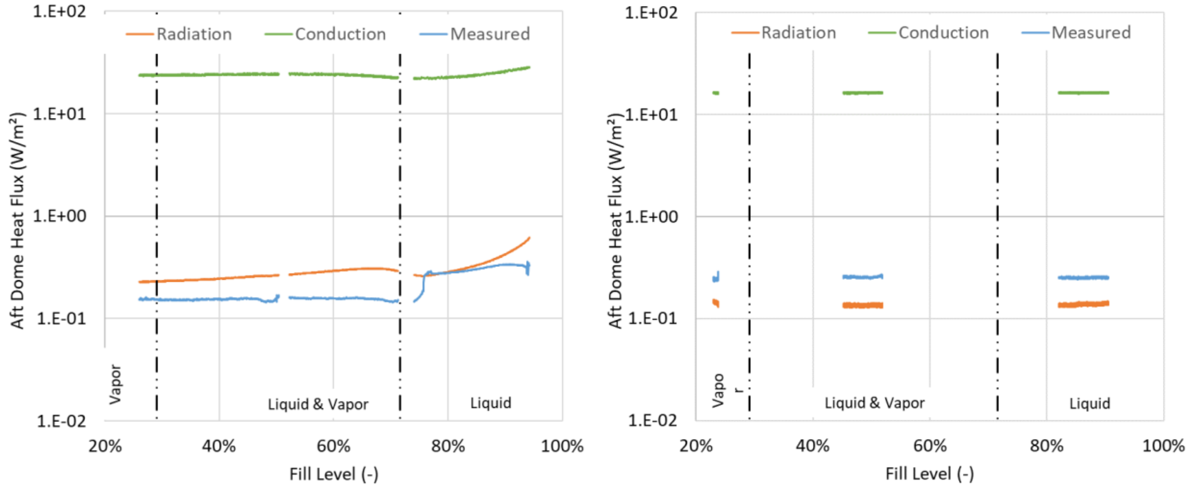

Figure 6. Aft dome heat flux calculations and measured hydrogen boil-off (left) and nitrogen vapor cooling (right).

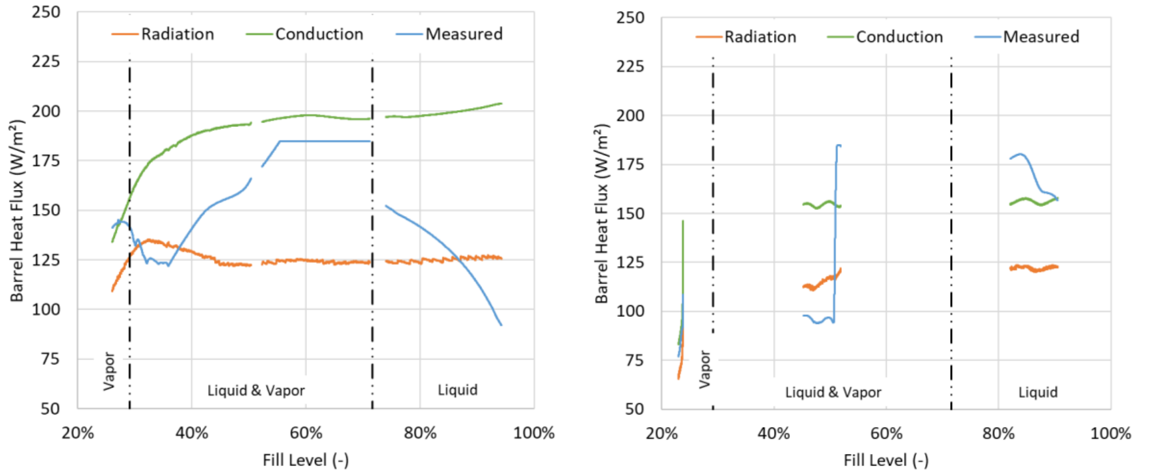

Figure 7. Barrel heat flux calculations and measured hydrogen boil-off (left) and nitrogen vapor cooling (right).

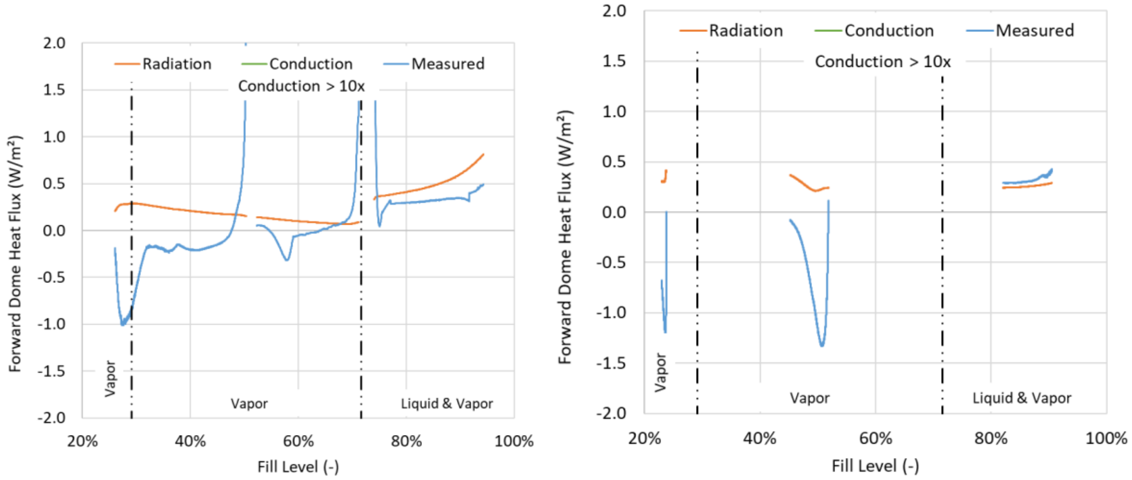

Figure 8. Forward dome heat flux calculations and measured hydrogen boil-off (left) and nitrogen vapor cooling (right).

On the forward dome in figure 8, the heat flux measurements show significant negative heat fluxes in several locations, especially at less than 70% full and coming out of a self-pressurization test. These indications are not seen in the radiation calculations. Figure 9 shows that at low fill levels, the forward flange (between the forward skirt and the tank) was the warmest part of the tank wall, while SD-21 was the coldest. This would indicate that the hydrogen vapor is absorbing heat off of the flange and transporting it to the top of the dome, warming it up in addition to conduction up the dome wall. Perhaps the heat flux sensors are picking up on this non-one-dimensional heat transfer in the system and truly reading a negative heat flow (from the dome wall into the SOFI) with heat also flowing from the MLI into the SOFI (giving the indication of the radiation calculation).

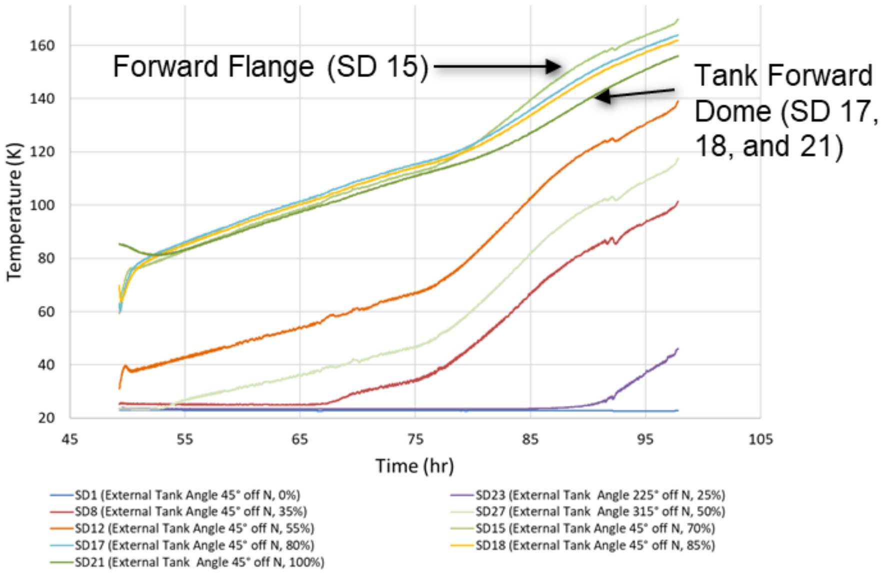

Figure 9. Forward dome temperature gradients during liquid hydrogen boil-off testing at low fill levels.

5. Conclusions

Testing of the heat flux sensors on the SHIIVER tank with both hydrogen and nitrogen give an interesting set of results. The heat flux sensors measure the appropriate order of heat flux coming into the system, both at 100 W/m^2 and at less than 1 W/m^2. Additionally, they provide general indication of the direction of flow and relative steadiness of the heat flow in the system at the point location they are at. While the uncertainty of the heat flux sensors used on SHIIVER is fairly high, the development of or improvement of heat flux sensors specifically for cryogenic applications and low heat fluxes would be of interest for use in complex systems for trouble shooting and gaining a better understanding of the system performance.

6. References

[1] Johnson W L, Balasubramaniam R, Hibbs R, et. al., Demonstration of Multilayer Insulation, Vapor Cooling of Structure, and Mass Gauging for Large-Scale Upper Stages: Structural Heat Intercept, Insulation, and Vibration Evaluation Rig (SHIIVER) Final Report, NASA TP 2020-5008233, 2021.

[2] Johnson W L, Balasubramaniam R and Westra K, Testing of Heat Flux Sensors at Cryogenic Temperatures, IOP Conf. Ser. Mater. Sci. Eng., vol. 755, no. 012074, 2020.

[3] Fesmire J E, Aerogel insulation systems for space launch applications, Cryogenics, vol 46, Issue 2-3, 2006, 111-117.

[4] Barrios M S and Van Sciver S W, Thermal conductivity of rigid foam insulations for aerospace vehicles, Cryogenics, vol 55-56, 2013, pg 12 – 19.

[5] Black I A and Glaser P E, "Progress Report on Development of High-Efficiency Insulation," in Advances in Cryogenic Engineering, Vol 6 , Boulder, CO, National Bureau of Standards, 1961, pp. 32-41.

[6] Srinivasan J, A paradox in radiation heat transfer, AIP Advances, pages 85-91, 2007.

[7] Elchert J P, Cryogenic Multilayer Insulation Theory and an Analysis of Seams Assuming Spherical Blankets Under a Variety of Assumptions, Master's Thesis, Cleveland State University, Dec 14, 2017

Acknowledgements

This work was funded by the Evolvable Cryogenics Technology Demonstration Mission, a project within the Space Technology Mission Directorate of the National Aeronautics and Space Administration.

The authors would like to acknowledge Mr. Joseph Zoeckler for his suggestions, research, and leg work to make sure the heat flux sensor measurements were realized.